VTT Technical Research Centre of Finland

Experimental and techno-economic analysis of solar-assisted heat pump drying of biomass

Thomasson, Tomi; Raitila, Jyrki; Tsupari, Eemeli

Published in:
Energy Reports

DOI:
10.1016/j.egyr.2023.11.062

Published: 01/06/2024

Document Version
Publisher's final version

Energy Reports 11 (2024) 316–326

Contents lists available at ScienceDirect

Energy Reports

journal homepage: www.elsevier.com/locate/egyr

Research paper

Experimental and techno-economic analysis of solar-assisted heat pump drying of biomass

Tomi Thomasson *, Jyrki Raitila, Eemeli Tsupari

VTT Technical Research Centre of Finland Ltd, Koivurannantie 1, 40101 Jyväskylä, Finland

ARTICLE INFO

Keywords:
Biomass
Solar drying
Hybrid drying
Economic feasibility
Heat pump
Optimization

ABSTRACT

Drying enhances the attributes of biomass, such as storability and heating value. In regions with low solar radiation, solar drying has demonstrated limited economic viability. Hybrid systems, combining solar drying with a stable heat source such as a heat pump, present an opportunity to improve drying performance and achieve cost savings, especially with time-variable electricity pricing. To quantify this potential, we constructed an experimental drying system in Finland, incorporating an air-source heat pump and solar thermal collectors for drying woody biomass. Experimental work, consisting of 316 h of operation in varied conditions, evaluated the performance of the hybrid drying system. Subsequently, we developed data-driven models to estimate drying rates and power consumption in both hybrid and solar operation modes. Finally, these models were integrated into a techno-economic optimization model to assess the economic feasibility of the concept through hourly simulations. Hybrid drying experiments resulted in a significantly improved average drying rate (33.0 kg/h ± 5.4 kg/h) compared to solar drying (9.0 kg/h ± 3.2 kg/h) with a 45% increase in specific electricity consumption. The experimental work also revealed limited operating flexibility in colder temperatures due to an exponentially increasing preheating time (up to 4.2 h at 0 °C). With techno-economic modelling, the simulations yielded a simple payback time of 7.5 years for a commercial-scale drying system without investment subsidies. Applying an optimized operating strategy, system operation shifted on average from hybrid mode (96–33%) to solar mode (3–36%) and inactive state (1–31%) with an increased electricity price level, highlighting the need for advanced operation planning. Commercial deployment should prioritize use cases with high value increase through drying or obtaining compensation from avoided biogenic CO_2 emissions through drying, as these two parameters were shown to have the greatest impact on the investment payback time.

1. Introduction

Climate change mitigation calls for urgent measures to substitute fossil fuels and materials with renewable solutions. Currently, biomass represents roughly 10% of the global primary energy supply. However, there is a need for further expansion, as a 10% annual increase in deployment until 2030 is required to align with the IEA's Net Zero Scenario (IEA, 2023). Furthermore, to meet the climate targets set for 2050, a more substantial increase in biomass deployment will be required (Mandley et al., 2020). Recent national-level studies have recognized the role of bioenergy as an important component in system design, including as part of a diverse portfolio of technology solutions (Lund et al., 2022), to retrofit existing coal-fired power plants (Yang et al., 2022), and in areas where direct electrification is challenging (Xing et al., 2021). Furthermore, with the increasing share of variable renewable energy, bioenergy offers flexibility potential on both short-term and seasonal levels due to its dispatchability and bioenergy carrier storage capabilities (Schipfer et al., 2022). In short term, biomass plays a significant role in the European Union, where several countries have committed to phase out coal before 2030 (European Investment Bank Group, 2020). In Finland, where coal-fired power and heating generation will be banned as of May 2029 (Finnish Government, 2019), the simultaneous rapid decrease in the use of fuel peat in combined heat and power production due to high CO_2 emissions allowance prices has already been estimated to lead to substantial increase in biomass demand (AFRY, 2020). However, sustainable biomass resources are limited, and the carbon neutrality of some biomass fractions has been questioned (Agostini et al., 2013).

Biomass drying can contribute to the utilization of bioenergy. From a technical perspective, drying wood-based biomass below 25 w-% moisture content helps prevent the loss of quality and dry matter

* Corresponding author.
E-mail address: tomi.thomasson@vtt.fi (T. Thomasson).

https://doi.org/10.1016/j.egyr.2023.11.062
Received 29 September 2023; Received in revised form 13 November 2023; Accepted 29 November 2023
Available online 7 December 2023

Nomenclature

Acronyms

ANN	Artificial neural network
BOD	Benefit of drying
COP	Coefficient of performance
MAE	Mean absolute error
OPEX	Operating expenditure
PBT	Payback time

Superscripts

act	active
dry	after drying
el	electricity
in	income
inv	investment
obj	objective
rem	removed
w	water
wet	before drying

Subscripts

i	operating mode
j	input parameter
N	set of operating modes
M	set of input parameters
t	time
T	set of hours

Symbols

a	coefficient
c	input parameter
C	cost €
$\dot{m}$	drying rate kg/s
M	coefficient
p	specific cost €/MWh, c/kWh
P	electricity consumption kWh
Q	lower heating value MWh/kg
x	binary variable

through biodegradation (Krigstin and Wetzel, 2016). In addition to the quality improvement, reduction of moisture content can also increase the economic value of biomass, as the lower heating value of the fuel increases (Demirbas, 2002; Pang and Mujumdar, 2010). Furthermore, the CO_2 emission factor of a biomass fuel decreases through drying (Svoboda et al., 2009). Although biogenic CO_2 emissions are currently not considered greenhouse gas emissions in the EU Emissions Trading System, a potential regulation change or voluntary carbon markets could increase the value of dried biomass. Finally, from a system perspective, biomass drying contributes to increasing resource sufficiency, as solar energy available during summer can be shifted to winter, aligning better with the energy demand, and by diminishing risks in biomass fuel delivery (Sharma et al., 2009). This study is continuation of the work by Raitila and Tsupari (2020), who investigated solar-enhanced drying of woody biomass in Finland. Based on their experimental findings, a simple payback time of 12–17 years was estimated achievable when upscaling the drying system to a biomass terminal scale. However, without investment subsidies and at a smaller scale, the estimated payback time exceeded 30 years. To address this, the integration of a heat pump into the system for enhanced convective air drying was proposed as an improvement. This integration presents significant advantages especially in the Nordic climate where solar radiation availability is relatively high only during the summer. By incorporating a heat pump, the feasible annual operating time can be substantially increased, potentially leading to a reduction in the investment payback time.

In the field of drying research, the utilization of heat pumps has been extensively investigated since the 1970 s (Colak and Hepbasli, 2009). More recently, hybrid concepts that combine heat pumps with solar energy have gained attention, demonstrating improved drying performance compared to standalone solar drying. Despite their wide applicability in different industries, the developed types of these hybrid systems have been considered limited (Zou et al., 2023). Xie et al (2021) developed a TRNSYS model and conducted experimental work on solar-assisted heat pump drying, utilizing an air-water heat pump. Their study, focusing on carrots as the experimental material, achieved a 28.6–33.3% reduction in drying time compared to conventional solar drying, resulting in an estimated investment payback time of five years. Li et al (Li et al., 2021) explored the use of a solar-assisted air-source heat pump in the drying of medicinal materials in China. The constructed drying system exhibited an 80% increase in the coefficient of performance (COP) during hybrid operation compared to heat pump drying. Khouya (Khouya, 2021) developed a mathematical model for the drying of woody biomass using a hybrid system comprising a solar air collector and an air-water heat pump. Simulation conducted under the climate conditions of Morocco demonstrated drying time reductions of 24–52% when compared to a conventional drying system. Additionally, in the same climate, Khouya (Khouya, 2022) investigated a hybrid system for wood drying that integrated an air-water heat pump with a concentrated photovoltaic thermal system. The integration of solar energy resulted in an 18% reduction in drying time. Yao et al (Yao et al., 2023) analyzed a vacuum tube solar collector coupled with an air-source heat pump for drying of grapes, using three operation modes based on solar radiation availability. With combined heat pump and solar operation, the COP was increased by 44.2% and the average hourly power consumption decreased by 35% compared to heat pump drying.

Due to non-linear nature of drying, various modelling approaches for operational analysis have been developed, including kinetic models and artificial neural network (ANN) models. Gebgeegziabher et al (Gebgeegziabher et al., 2013) proposed a method based on Fick's second law of diffusion, which accurately estimates moisture removal for short drying periods. Francik et al (Francik et al., 2018) employed ANN models to simulate the drying of willow. Using experimental data from a convective dryer, the study developed separate models for predicting water content, temperature, and mass of the wood chips. Kumar et al (Kumar et al., 2023) focused on a constructed forced convective cabinet solar dryer and developed an ANN model to assess the drying performance for three types of wood fuels. Their model incorporated various parameters such as weather conditions (solar radiation and relative humidity), dryer inlet and outlet temperatures, and initial moisture content. Moheno-Barrueta et al (Moheno-Barrueta et al., 2021) employed an ANN model coupled with an optimization algorithm to analyze the drying process in a forced ventilation solar dryer for agricultural products. The approach allowed for determining the optimal drying velocity, with input parameters comprising weather conditions (solar radiation, ambient temperature, relative humidity, and wind velocity), as well as dryer input and output temperatures and fan voltage.

Based on the reviewed studies, a comprehensive evaluation of the economic feasibility of a hybrid heat pump and solar drying system has yet to be conducted for biomass fuels. In particular, the previous studies have not examined the economic aspects involved in the operational planning of the hybrid drying systems, despite their increasing significance in the context of market areas with time-variable electricity pricing. Therefore, this study aims to address this gap by demonstrating

and evaluating the economic feasibility of a hybrid biomass drying system combining a heat pump and solar thermal collectors. Building on the work of Raitila and Tsupari (Raitila and Tsupari, 2020), the performance of the system is assessed through a multitude of drying experiments. Subsequently, a short-term optimization model is developed with an approximation of drying rate and power consumption using gradient boosting and linear regression techniques. Finally, to evaluate the economic feasibility of the drying system with optimized operating strategies, techno-economic modeling is employed. This analysis encompasses various price assumptions and considers additional income formation mechanisms such as investment subsidies and income from avoided biogenic CO_2 emissions. The overall structure and research methodology of the study is summarized in Fig. 1.

2. Materials and methods

2.1. Studied drying system

The experimental drying system was built into two 20-foot (6 m) freight containers. The first container contains a 24 kW (maximum thermal output) heat pump by Rivacold, condenser, evaporator, heat recovery unit and heat exchanger, all integrated into an industrial air supply unit, manufactured by Koja Ltd. Twelve flat-plate solar heat collector modules, provided by Sundial Ltd., with a total collector surface area of 24 m^2 corresponding to roughly 22 kW_{th}, were installed on the roof and one side of the container (Fig. 2A). The main role of the heat pump is to remove moisture from the drying air, but it can also provide additional heat in the beginning of the drying process, since to work efficiently, the drying air temperature must reach at least 20 °C before switching the heat pump into a drying mode. Heat is transferred with water-glycol fluid, which is pumped to the heat exchanger, placed in front of the inlet air duct. All solar thermal collectors were positioned to face south with 45° inclination. The second container (Fig. 2B) functions as a drying chamber. Biomass is dropped onto a perforated floor through a hatch in the roof. The container is inclined about 40 degrees, which enables bottom scrapers to move biomass downwards. From the lower end, biomass can be circulated back with a rotating chain conveyer. Biomass is removed from the dryer with the same conveyors. Drying air is blown through the biomass layer from below through the perforated floor.

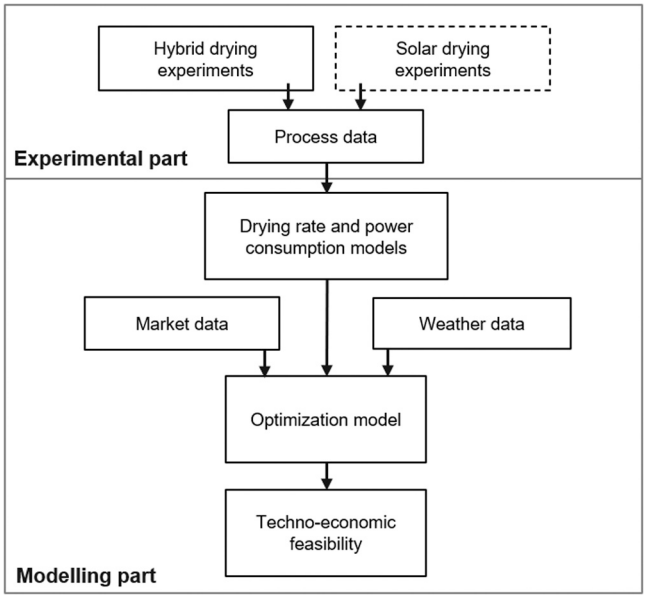

Fig. 1. The overall structure of the study divided into experimental and modelling parts. For solar drying experiments, the process data is acquired from previous work (Raitila and Tsupari, 2020).

Three different drying modes can be utilized with the hybrid drying system (Fig. 3). The first is closed loop drying, where the same air is continuously circulated through the system. Moisture is removed in the air supply unit using evaporator of the heat pump, while the condenser provides heat. Second, when solar radiation is available, the solar thermal collectors provide an additional heat input, making both the heat pump and solar loop operational. Third, the solar loop can also be used independently, in which case the entire heat input is provided by the solar thermal collectors. In this case, the heat pump is switched off, and all moist air is vented out of the system while fresh air is introduced for the drying process. The operation of the heat pump is controlled by the manufacturer's control device, which optimizes the suction and condensing pressures within predetermined limits. In the subsequent sections, we refer to the operation in the first and second operating modes as hybrid, while the operation in the third operating mode will be referred to as solar.

Throughout the experiments, the drying system was operated manually. We established maximum and minimum limits for the fluid temperature in the condenser as a part of the control strategy based on drying experiments and recommendations of the manufacturer. When the temperature exceeded 70 °C, the heat pump was deactivated, and hot moist air was ventilated out. Conversely, when the condenser temperature decreased below 50 °C, the heat pump was activated and the closed loop drying continued. As the heat pump cannot function with high condenser temperatures, pausing the heat pump enables safe operation in addition to conserving electricity, and under certain weather conditions, speeds up the drying process.

2.2. Experimental setup and regression models

Hybrid drying experiments were conducted with the described drying system during 2021 and 2022 from March to November. The coldest months were excluded, as the drying system is lightly insulated and designed to work in temperatures above −5 °C. For the drying experiments, fresh wood chips in size classes P16 and F15 (International Organization for Standardization, 2014) were used. The wood chips were manufactured from small-diameter (7–15 cmbh) birch logs by chipping with an agricultural tractor-powered disc chipper. The average batch size of wood chips in the experiments was 1046 kg (682–1770 kg). The goal was to dry the wood chips to a moisture content between 20 and 30 w-%.

Continuous process measurement data from 316 h of operation was averaged into ten-minute frequency. The available process measurements included different air flows (Nm^3/h), relative humidity of incoming and exhaust air (%), temperature of incoming and exhaust air (°C), power consumption of fans, heat pump and other drying container equipment (W), and irradiation on a horizontal surface (W/m^2). For completeness, the data were further enriched with air temperature (°C), relative humidity (%) and solar irradiation (W/m^2) measurements from the nearest weather station of Finnish Meteorological Institute (Finnish Meteorological Institute, 2023), located roughly 20 kilometers from the drying system. For comparison, similar data for solar drying experiments were retrieved (Raitila and Tsupari, 2020). The experimental conditions in terms of mean air temperature and total water removal are summarized in Fig. 4.

From the enriched process data, models were developed to estimate the drying rate and power consumption in different operating conditions. For hybrid drying, a gradient boosting model for drying rate was implemented with LightGBM (Ke et al., 2017) and trained using only parameters external to the process as the input. For the power consumption, a multiple linear regression model with drying rate and parameters external to the process were used as the input. To improve the model accuracy, for the hybrid drying experiments, the process measurement data were divided manually into preheating and drying sections based on the measured drying rate and temperature of exhaust air.

Fig. 2. The experimental hybrid drying system (a), consisting of two containers with air ducts between them, and the drying chamber (b), in which biomass is placed on the scrapers on the perforated floor and the circulating conveyer is seen on the ceiling.

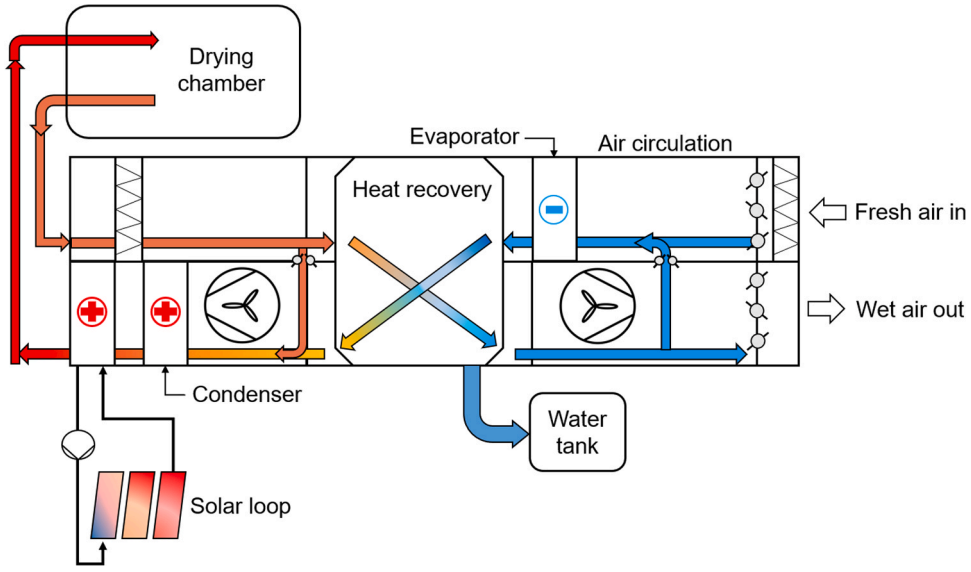

Fig. 3. Flowsheet of the hybrid drying system used in the study.

For solar drying, a single-parameter linear model was employed for power consumption based on inlet fan speed setpoint, and a multiple linear regression model for drying rate. The model formulation, including the regression model coefficients, is summarized in Table 1.

2.3. Techno-economic model

To assess the economic feasibility of the optimal dryer operation, an hourly short-term optimization model was developed. The model is formulated around the drying rate, for which the hourly maximum value ($\dot{m}^{w,max}$) is determined either from regression model (solar, (Eq. 1)) or gradient boosting model (hybrid) based on the regression model coefficients (a) and hourly parameter values (c). With the calculated water removal, the associated power consumption P (Eq. 2) can be determined using the respective regression model. To determine the operating income, the benefit of drying p^{BOD} (Eq. 3) is defined by assuming an increased value for dried biomass due to improved quality, better storability, and lower transportation costs. Therefore, the benefit of drying can be calculated based on the initial and target heating values and the respective biomass costs. Additionally, operating income can be formed indirectly from the increased biogenic carbon content if a value (for such is assumed. Thus, the total operating income (C^{in}) can be formulated as in (Eq. 4). The total operating cost (C^{OPEX}) is formed based on the electricity consumption of the active operating mode (Eq. 5). The objective function of the model is defined as in (Eq. 6). In addition, simple payback time C^{PBT} (Eq. 7) is used to evaluate the feasibility of the investment.

$$\dot{m}_{t,i}^{w,max} = a_0 + \sum_{j=1}^{M} (a_j \cdot c_j) \quad (1)$$

$$P_{t,i} = a_0 + \sum_{j=1}^{M} (a_j \cdot c_j) \quad (2)$$

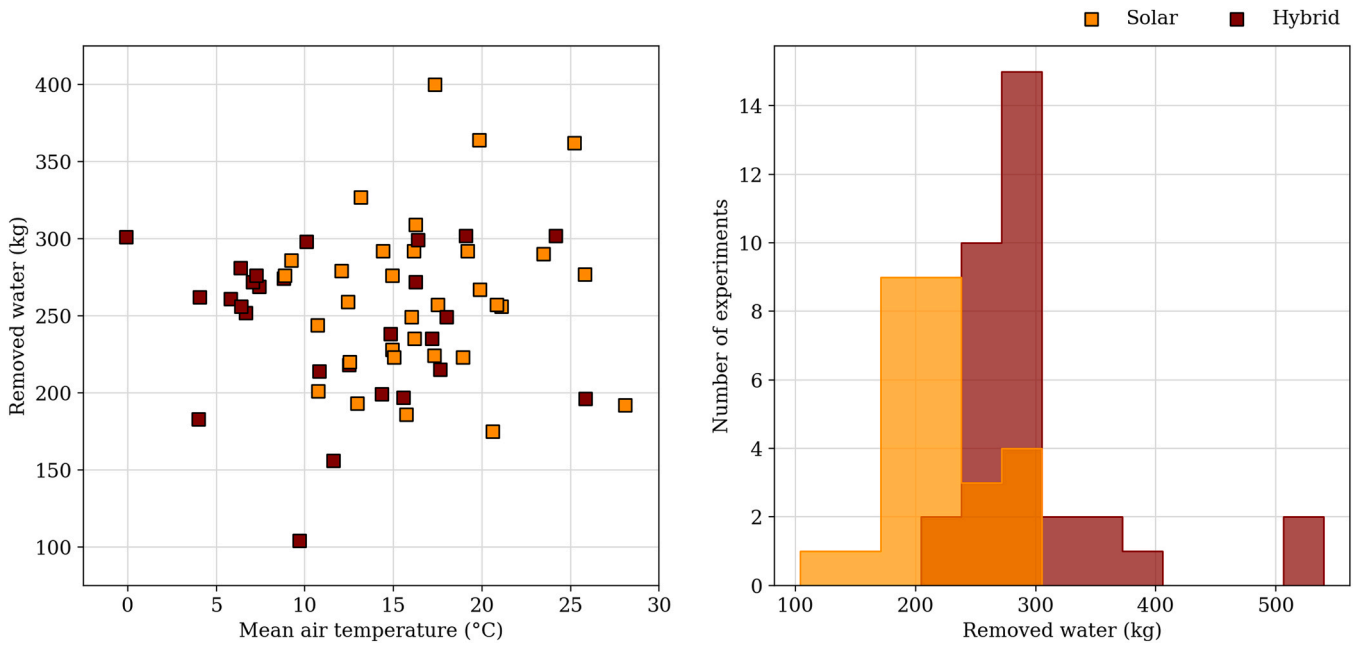

Fig. 4. Summary of the drying experiments: removed water as a function of mean air temperature during the experiment (left) and distribution of water removal (right) in the experiments.

Table 1
Model formulation for power consumption and drying rate in hybrid and solar operating modes. Regression model coefficients are shown where applicable.

Parameter	Hybrid	Solar
Power consumption		
Solar radiation (W/m^2)	$2.58{\cdot}10^{-5}$	$y = 0.02632 \cdot$ fan speed
Air temperature (°C)	− 0.0525	setpoint (%)
Relative humidity (%/100)	− 1.806	
Drying rate (kg/10 min)	0.962	
Intercept term	6.184	
Drying rate		
Solar radiation (W/m^2)	Gradient boosting	$1.819{\cdot}10^{-3}$
Air temperature (°C)	model used	$7.609{\cdot}10^{-3}$
Relative humidity (%/100)		− 2.356
Fan speed setpoint (%)		$6.503{\cdot}10^{-3}$
Intercept term		1.750

$$p^{\mathrm{BOD}} = \left(p^{\mathrm{dry}}{\cdot}Q^{\mathrm{dry}} - p^{\mathrm{wet}}{\cdot}Q^{\mathrm{wet}}\right) \Big/ \left(Q^{\mathrm{dry}} - Q^{\mathrm{wet}}\right) \tag{3}$$

$$C^{\mathrm{in}} = \sum_{t=1}^{T} \dot{m}_{\mathrm{t}}^{\mathrm{w,rem}} \cdot \left(p^{\mathrm{BOD}} + p^{\mathrm{CO2}}\right) \tag{4}$$

$$C^{\mathrm{OPEX}} = \sum_{t=1}^{T} \sum_{i=1}^{N} P_{\mathrm{t,i}} \cdot p_{\mathrm{t}}^{\mathrm{el}} \tag{5}$$

$$C^{\mathrm{obj}} = C^{\mathrm{in}} - C^{\mathrm{OPEX}} \tag{6}$$

$$C^{\mathrm{PBT}} = \frac{C^{\mathrm{inv}}}{C^{\mathrm{in}} - C^{\mathrm{OPEX}}} \tag{7}$$

The boundaries for water removal are defined by the biomass moisture content. The initial moisture content is used as an input, and the drying is continued until the target moisture content is within the specified acceptable range. To facilitate continuous drying, binary variables (x^{act}) are employed to activate the operating mode (Eq. 8), determining the current drying rate $\dot{m}^{\mathrm{w}}$ (Eq. 9), which is bounded by the maximum value (Eq. 10). The remaining water to be removed, $\dot{m}^{\mathrm{w,left}}$ (Eq. 11) is calculated based on its previous value, the current drying rate, and an additional variable that manages water removal ($\dot{m}^{\mathrm{w,rem}}$). Finally, the water removal is constrained (Eq. 12) by a binary variable (x^{rem}) and the water content determined from the acceptable range of target moisture content ($\dot{m}^{\mathrm{w,rem,min}}$, $\dot{m}^{\mathrm{w,rem,max}}$). When activated, the removal of water simultaneously introduces a new batch of biomass (Eq. 11), which is computationally represented by an additional amount of water to be removed. A minimum uptime constraint is not imposed on the operating modes to encourage opportunistic use of the heat pump.

$$\sum_{i=1}^{N} x_{\mathrm{t,i}}^{\mathrm{act}} = 1 \tag{8}$$

$$\dot{m}_{\mathrm{t,i}}^{\mathrm{w}} \le M{\cdot}x_{\mathrm{t,i}}^{\mathrm{act}} \tag{9}$$

$$\dot{m}_{\mathrm{t,i}}^{\mathrm{w}} \le \dot{m}_{\mathrm{t,i}}^{\mathrm{w,max}} \tag{10}$$

$$\dot{m}_{\mathrm{t,i}}^{\mathrm{w,left}} = \dot{m}_{\mathrm{t-1,i}}^{\mathrm{w,left}} - \sum_{i=1}^{N} \dot{m}_{\mathrm{t,i}}^{\mathrm{w}} + \dot{m}_{\mathrm{t}}^{\mathrm{w,rem}} \tag{11}$$

$$x_{\mathrm{t}}^{\mathrm{rem}}{\cdot}\dot{m}^{\mathrm{w,rem,min}} \le \dot{m}_{\mathrm{t}}^{\mathrm{w,rem}} \le x_{\mathrm{t}}^{\mathrm{rem}}{\cdot}\dot{m}^{\mathrm{w,rem,max}} \tag{12}$$

2.4. Studied scenarios

Table 2 summarizes the default techno-economic parameters used in the optimization model. To reduce the complexity of the optimization problem, a representative day formulation was employed. Using k-means clustering, twenty representative periods of 48 h were selected from the electricity price and weather data. Hourly data spanning two years (2020 and 2021) was retrieved for the Finnish market area (ENTSO-E, 2023) for electricity prices and from the Finnish Meteorological Institute for weather data. The former year was considered as the baseline and the latter year used to evaluate the effect of a different electricity price profile. For sensitivity analysis, the electricity price datasets were uniformly upscaled to achieve the desired average electricity price. For biomass, the default price level was estimated using near-term historical price data from Statistics Finland (Statistics

Table 2
Default techno-economic parameters used in the optimization model.

Parameter	Value	Unit	Reference
Time-series data (2020/2021)			
Mean air temperature	6.0/7.1	°C	(Finnish Meteorological Institute, 2023)
Mean relative humidity	79.1/80.2	%	(Finnish Meteorological Institute, 2023)
Mean direct solar radiation	108.3/104.5	W/m^2	(Finnish Meteorological Institute, 2023)
Average electricity price	2.8/7.2	c/kWh	(ENTSO-E, 2023)
Standard deviation of electricity price	2.1/6.6	c/kWh	(ENTSO-E, 2023)
Basic economic parameters			
Electricity transmission cost	7	c/kWh	Own assumption
Biomass initial economic value	22	€/MWh	(Statistics Finland; Fastmarkets FOEX, 2020)
Biomass target economic value	26	€/MWh	Own assumption
Pilot-scale investment cost	85	k€	Calculation
Commercial investment cost	63	k€	Calculation
Weighted average cost of capital	6	%	Own assumption
Additional economic parameters			
Avoided CO_2 emission cost	50	€/t_{CO2}	(Statista, 2023)
Investment subsidy	30	%	(Centre for Economic Development, 2023)
Technical parameters			
Biomass batch size	500	kg	Own assumption
Initial moisture content	45	%	Own assumption
Target moisture content	24–28	%	Own assumption

Finland) and the PIX Forest Biomass Finland Index (Fastmarkets FOEX, 2020). For computational reasons, a biomass batch size of 500 kg was selected, allowing the possibility of drying the entire biomass batch in solar operating mode within the representative period.

The investment cost for the drying system was separately estimated for both the pilot-scale unit and a commercial unit. For the pilot-scale unit, the investment cost was determined based on the actual procurement cost, while for the commercial unit, the cost was estimated considering the economies of scale and a reduced instrumentation requirement compared to the pilot-scale unit. In certain scenarios, additional income derived from the reduction of biogenic CO_2 emissions through the drying process was considered. To estimate the economic value of these emission reductions, a specific cost of 50 €/t_{CO2} was employed. The price is equivalent to half of the near-term historical maximum price of fossil CO_2 emissions in the EU ETS (Statista, 2023), and could be achieved through, for example, voluntary carbon markets. In addition, an investment subsidy of 30% was considered for certain scenarios based on the available business development grant scheme in Finland (Centre for Economic Development, 2023).

3. Results and discussion

3.1. Experimental analysis

The drying performance in terms of average drying rate is shown in Fig. 5. With hybrid drying, an average end moisture content of 23.2% (16.0–28.1%) was achieved, corresponding to 21.9 w-% average reduction in moisture content. Compared to solar drying, hybrid drying increases the drying rate on average. Therefore, the wood chip batches are dried faster with a smaller variation in drying time. The average drying rates were 32.96 kg/h ± 5.36 kg/h (duration 9.3 h ± 3.27 h) with hybrid drying and 9.0 kg/h ± 3.19 kg/h (duration 26.1 h ± 7.54 h) with solar drying, corresponding to an increase of 366%. Since the initial water content and the total water removal vary in each experiment (refer to Fig. 4B), normalizing the average drying rates with respect to initial water content results in a 280% increase. The decreased drying duration is enabled with increase in the electricity consumption with the heat pump, being 8.24 kW ± 1.1 kW compared to 1.45 kW ± 0.46 kW. However, due to the improved drying rate, the specific electricity consumption in hybrid operation mode is only 45% higher at

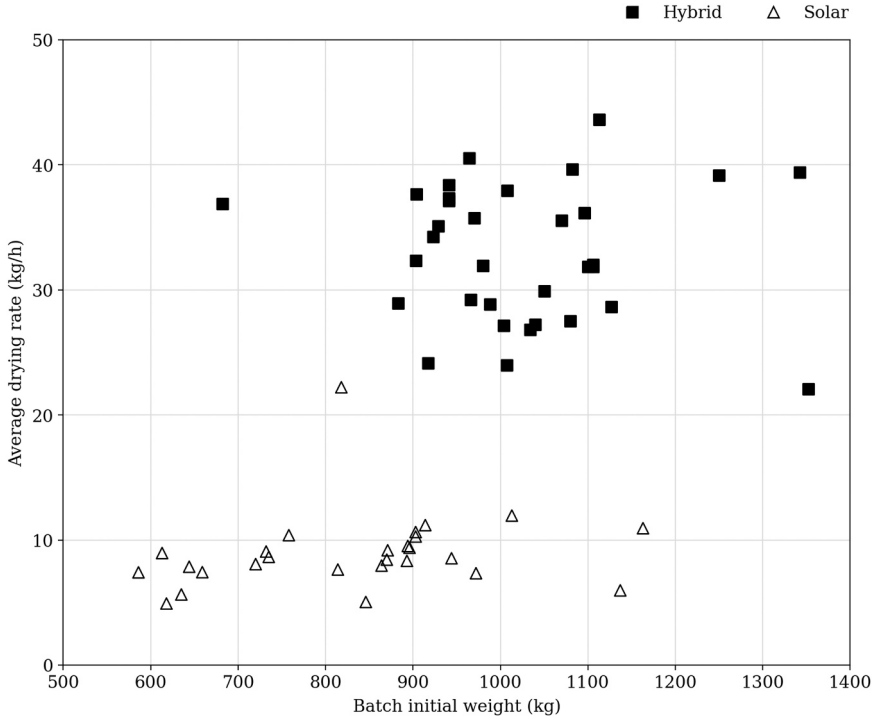

Fig. 5. Average drying rate of the hybrid and solar drying experiments.

0.26 kWh_e/kg compared to 0.18 kWh_e/kg. In hybrid operation, the drying rate shows relatively high positive correlation with average solar radiation ($R^2 = 0.74$) and air temperature ($R^2 = 0.74$), and negative correlation with relative humidity ($R^2 = 0.68$). Consequently, the highest average drying rate (43.6 kg/h) was achieved in an experiment with a combination of the three favorable parameter values (684 W/m^2, 27.8 °C, 29.0%).

The hybrid drying experiments show considerable correlation between required preheating time and air temperature. The required preheating time increases exponentially from 10 min (20 °C) to 70 min (10 °C) and to 250 min (0 °C). Consequently, as the electricity used for preheating increases linearly with time, the share of preheating of the total electricity consumption increases from 1% to 20% between the extreme air temperature values. Considering operating flexibility, the increased heating duration would not significantly affect the potential switching to solar drying, as relatively low amount of solar radiation is available in wintertime. However, the increased heating duration affects the potential flexibility of the heat pump operation, as the longer heating period must be considered when switching the heat pump off for a longer period, for example, to avoid peak electricity prices. In selected experiments, the heat pump was periodically switched off for 30 min (refer to Fig. 6B) to assess its impact on the drying performance. A slight decrease in the drying air outlet temperature, averaging 3 °C per 30 min, was observed. The drying air temperature was consistently maintained above 30 °C during steady drying conditions. Despite the temperature gradient indicating that the 20 °C limit, which necessitates preheating for the heat pump, would not be reached within an hour, it should be noted that the experiments were conducted exclusively during warm temperatures (21–30 °C).

3.2. Model validation

To assess the accuracy of the developed models for drying rate and power consumption, we conducted validation using measured data from the experiments. Fig. 6 provides an example of the validation process, presenting two hybrid drying experiments (a–b) and two solar drying experiments (c–d) under different experimental conditions, along with the corresponding drying rates. The data points used for model training are depicted in black, and the model predictions are shown in green with markers, while the remaining data points from the experiment are shown in gray. The quality of the models was evaluated based on the mean absolute error (MAE) and relative error. The drying rate model was developed using a calculated continuous measurement. The approach led to a slight error which could not be fully rectified, as the total calculated value slightly deviated from a physically measured value after each experiment due to leakages.

For hybrid drying, experiments with continuous (Fig. 6A) and discontinuous (Fig. 6B) heat pump operation are compared. In the latter, the heat pump was periodically switched off for 30 min. When considering all experiments, an average MAE of 0.27 (5.9%) for the drying rate and an average MAE of 0.88 (8.9%) for the power consumption was achieved. This accuracy was achieved by applying filtering to the training data. We excluded data points from the preheating period, periods when the heat pump was switched off, and final data points that were considered invalid. Consequently, as the model does not incorporate control parameters such as fan air flows, it is only capable of predicting stable drying situations with reasonable accuracy. For solar drying, Fig. 6C and Fig. 6D depict two experiments lasting approximately 24 h and 48 h, respectively. In comparison to hybrid drying, slightly higher average error was realized for the drying rate (0.24, 8.36%) and for the power consumption (0.20, 11.7%). The models were trained using a subset of the available data with relatively similar operating strategy in terms of fan utilization. Consequently, the accuracy of the models was improved by including a model parameter for the fan speed, which exhibited a high correlation with both the power consumption and the drying rate. However, due to the specific parameter selection, negative predicted values for the drying rate can be observed. These negative values are infeasible and are appropriately constrained within the optimization model.

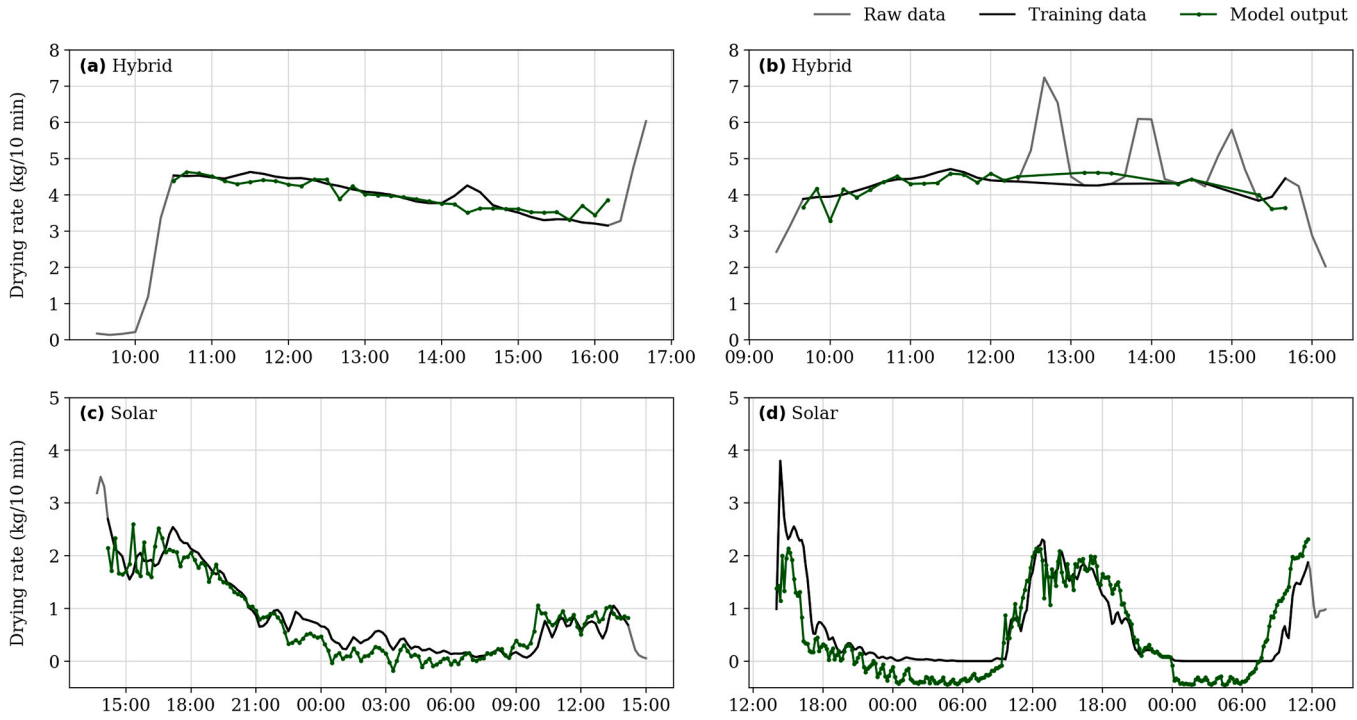

Fig. 6. Drying model validation: comparison of raw data, training data and model output for four different experiments in hybrid operation (a–b) and solar operation (c–d).

3.3. Economic feasibility

To assess the economic feasibility of the drying system, simple payback time for the investment is calculated using the optimization model considering three varied parameters and their combinations: the value increase of biomass in drying, the cost of biomass, and the average price of electricity. Fig. 7 shows the results with commercial investment cost assumptions. With reference parameter values, marked with a black circle, the payback time is 7.5 years. With pilot-scale investment cost assumptions, the payback time is 10.1 years. Compared to the reference study with the most similar conditions (Raitila and Tsupari, 2020), the results show a significantly shorter payback time. In their research, the payback time exceeded 30 years without the support of investment subsidies or economies of scale. The improved economic feasibility can be attributed to a substantial enhancement in drying performance achieved through hybridization. This improvement, shown to be 280% with normalized average drying rates, is higher than reported in the studies conducted for woody biomass by Khouya (Khouya, 2021, 2022) or to other materials by Xie et al (Xie et al., 2021). and Yao et al (Yao et al., 2023). The higher improvement compared to literature can be explained by the relatively weaker baseline performance of the drying system, influenced by the limited availability of solar radiation in our specific context.

Fig. 7 reveals that the drying value increase has the most significant impact on the payback time (1.09%/%), followed by the cost of biomass (0.62%/%) and the price of electricity (0.54%/%), when determining the value change over parameter value change. The parameters and their effects are interdependent. For example, when the drying value increase is low (2 €/MWh), changes in the average price of electricity or the cost of biomass can lead to greater variation in the payback time. As extreme parameter combinations (e.g., low electricity price and high biomass valuation) are less likely to occur, the respective extreme low and high payback times are less realistic. With a 30% investment subsidy, the payback times decrease to 7.1 and 5.3 years for the pilot and commercial scales, respectively, corresponding a sensitivity of 2.04%/%. Alternatively, with a biogenic CO_2 compensation, the payback times decrease to 6.5 and 4.8 years. Lastly, by replicating the simulation with the data of the alternative simulation year (2021), we find that the increased electricity price variation has a relatively small effect on the payback time, decreasing the value on average by 3.5%.

Fig. 8 expands on the economic analysis by displaying the annual cost and income structures of selected scenarios. Specifically, the reference scenario is compared with three alternatives: an increased value of drying (6 €/MWh), an increased biomass price (50 €/MWh), and the inclusion of biogenic CO_2 compensation. The results are shown for three different average electricity prices, with the annual net profit indicated by a horizontal marker. Fig. 8 also includes the cost of capital to show the annual investment payment, in contrary to the earlier results. Additionally, the secondary horizontal axis displays the annual total drying amount. The annual net profit is directly correlated with the total drying amount, with fewer biomass batches being dried as the average electricity price increases. In the reference scenario, 52% less biomass is dried annually. Consequently, the income from drying decreases and the operating cost shifts from hybrid drying to solar drying. This effect is observed across all scenarios regardless of the parameter assumptions: the increased biomass price scenario leads to a 44% reduction in the amount of biomass dried, while the increased drying value and biogenic CO_2 compensation scenarios both result in a 40% reduction.

Although the changes in the three scenarios lead to an increase in the number of feasible operating hours in comparison to the reference scenario, the cost structures are not drastically changed. However, the break-even electricity price increases from 16.2c/kWh (reference) to a maximum of 25.7c/kWh (increased drying value), indicating that a favorable investment environment could enable feasibility at a considerably higher electricity price level. Additionally, the total drying

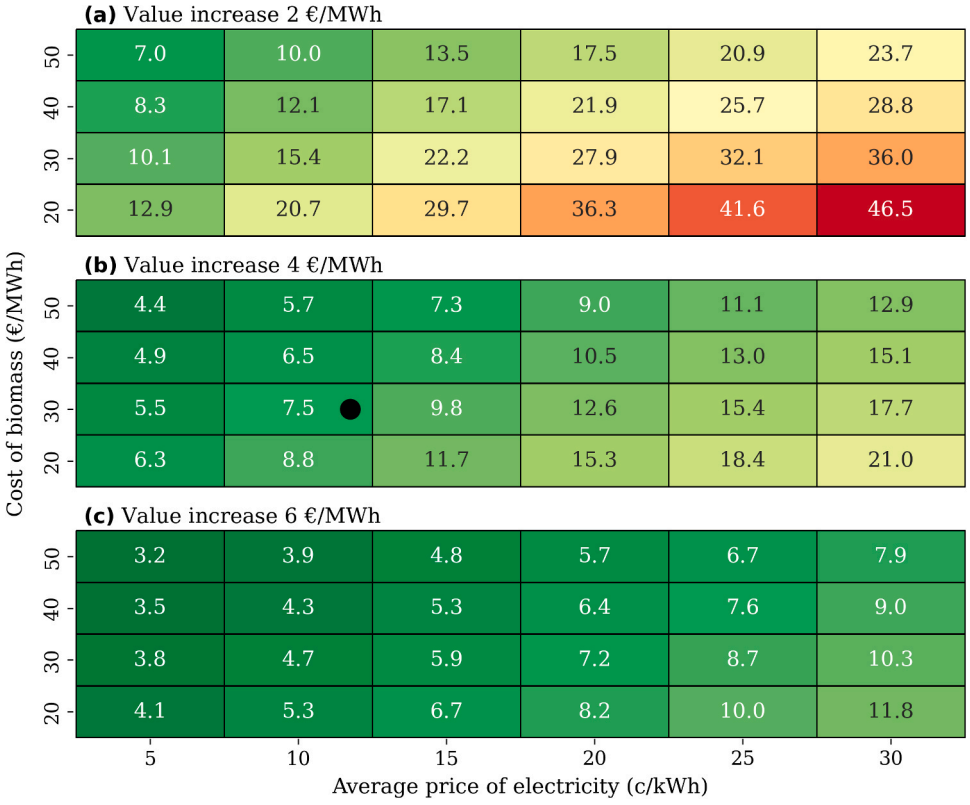

Fig. 7. Simple investment payback time (in years) for the hybrid drying system with commercial-scale cost assumptions. The x-axis represents the average price of electricity, and the y-axis represents the cost of biomass. The value increase of drying is varied in the different subfigures.

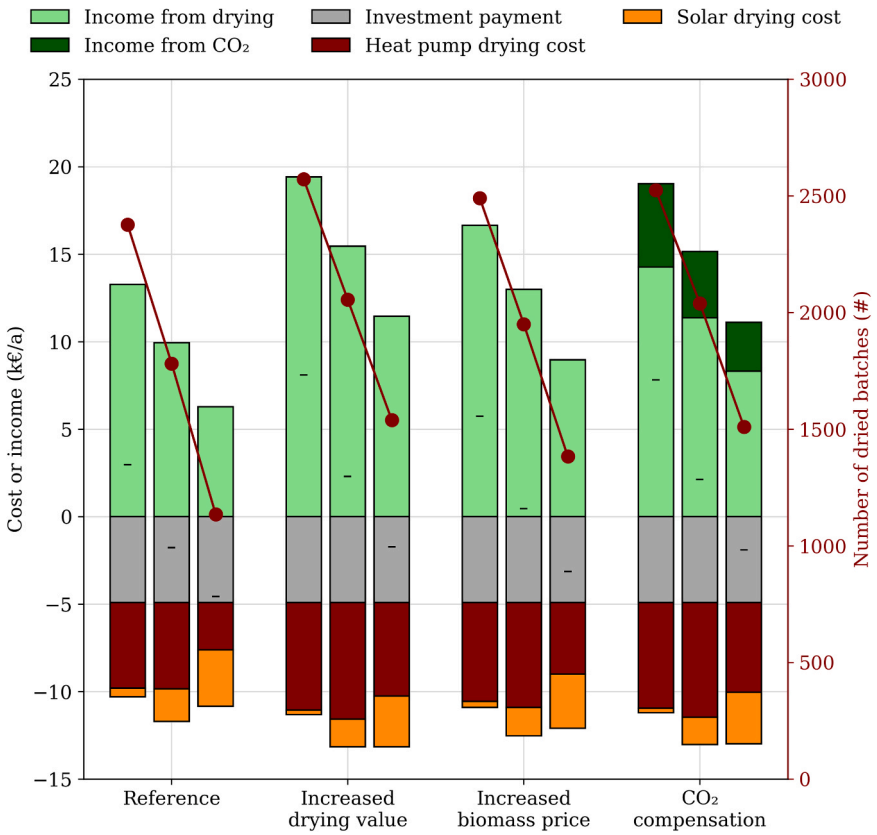

Fig. 8. Cost structures (bar) and total drying amount (line) for selected scenarios and three average electricity prices (10c/kWh, 20c/kWh and 30c/kWh) with commercial-scale cost assumptions.

amount should be considered. As the results show the economically optimal drying amount, increasing the drying requirement would decrease the economic feasibility of the system. In practice, the drying system may be under a contractual obligation to provide a certain amount of dried biomass, which would result in operation under non-profitable hours.

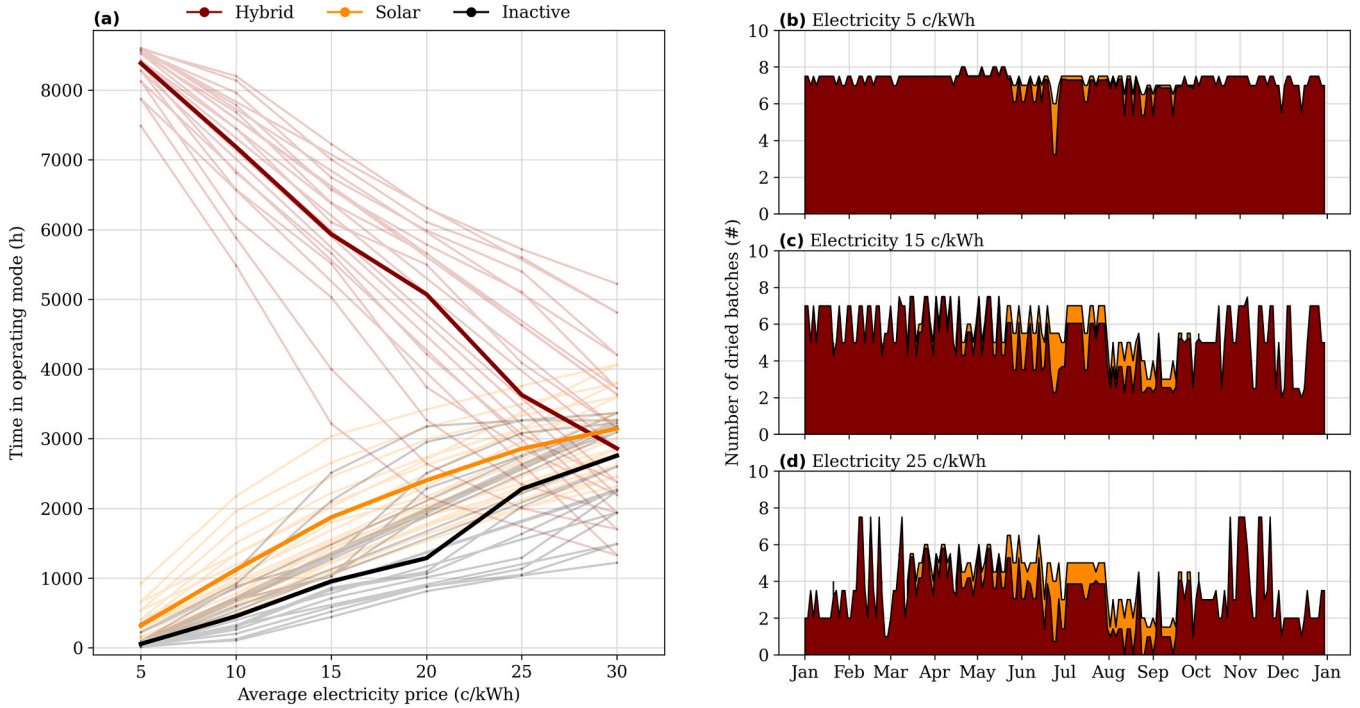

Fig. 9. Time (hours) in different operating modes as a function of average electricity price (a) and the number of dried biomass batches per day in three average electricity price scenarios: (b) 5c/kWh, (c) 15c/kWh and (d) 25c/kWh.

3.4. Annual operating strategies

To analyze optimal operating strategies at a broader level, Fig. 9 displays the annual operating time for different drying modes (Fig. 9A). Bold lines represent scenarios with reference parameters, while weaker lines indicate scenarios with varied parameter assumptions. In addition, Fig. 9B–9D illustrate the daily operation in terms of the number of dried biomass batches in different operating modes for three electricity prices with reference parameter assumptions. The comparison of daily operation reveals distinct operating regions. At lower electricity prices (<10c/kWh), drying is mainly conducted in the hybrid mode (96% at 5c/kWh), with support from solar drying during the summer (3%), and the number of inactive hours is low (1%). This region is followed by a transition period (10–20c/kWh), where solar operation increases, particularly in the midsummer, while hybrid operating hours steadily decrease. Consequently, due to lower drying rate, the average drying duration of a biomass batch increases from 3.3 h (at 5c/kWh) to 6.8 h (at 20c/kWh). In the final region (>20c/kWh), the number of inactive hours increase more rapidly due to the increased electricity price. Simultaneously, despite the lower specific electricity consumption, the increase in the number of solar drying hours slows down due to limited availability of solar radiation in the new hours, mainly in the spring. At the highest price level (30c/kWh), the use of different drying modes is relatively balanced: hybrid (33%), solar (36%), and inactive (31%), requiring the most flexible operation. It should be noted that achieving the optimal annual operation and the presented economic feasibility necessitates drying system operation through the wintertime, requiring sufficient infrastructure.

4. Conclusions

The study examined the technical and economic potential of hybrid solar-assisted heat pump drying of biomass in Nordic conditions. The experimental configuration developed by Raitila and Tsupari (Raitila and Tsupari, 2020) was expanded by introducing a heat pump to the drying system and by developing an optimization algorithm, used in the economic analysis, for short-term operational planning. The key findings of the study can be summarized as follows:

1. The hybrid drying system offers a promising technical solution to enhance drying performance in conditions with limited solar availability. Experimentally, 34 hybrid drying experiments totalling 316 h of operation allowed the performance of the drying system to be verified. The average drying rate (33.0 kg/h ± 5.4 kg/h) was significantly improved in comparison to pure solar drying (9.0 kg/h ± 3.2 kg/h). Due to the improved drying rate, the specific electricity requirement of drying was only slightly higher (0.26 kWh_e/kg) than in pure solar drying (0.18 kWh_e/kg). This potential is expected to be applicable to other types of solid biomass.
2. The hybrid drying system can enable a low payback time in conditions with limited solar availability. The economic feasibility was shown to be the most dependent on the added economic value of drying, which is expected to be higher in scenarios where biomass availability is limited due to logistical or regulatory constraints. Under reference parameter assumptions, a simple payback time of 7.5 years was projected for a commercial-scale installation with reduced instrumentation requirements. In the studied investment environment, the payback time could be further reduced through current and potential subsidy mechanisms: with an investment subsidy (30%, 5.3 years) or if the biogenic CO_2 emissions avoided through drying could be monetised (4.8 years).
3. Operating flexibility is required to achieve the estimated economic feasibility but shown possible in the experiments. The flexibility potential was shown to decrease in colder temperatures due to an exponential increase in required preheating time. Based on the economic analysis, the benefit of operating flexibility increases with the electricity price, as the optimal operation shifts from nearly constant hybrid drying towards increased solar drying and non-operating hours.

For future research, we recommend two topics. First, the generalized operational models employed in this study could be further improved by a more detailed characterization of operating flexibility. This improvement would enable a control logic capable of predictively adjusting the operating modes based on short-term factors such as cloudiness and time-variable electricity pricing, potentially enabling further economic benefits. Second, models, as presented in this work, could be used to achieve a more accurate estimation of the added value of drying by considering downstream processes that utilize the dried biomass. This consideration would introduce new dynamics to the operational planning, allowing for the economic feasibility to be evaluated from a systemic perspective. Furthermore, this analysis should comparatively assess the economic feasibility of the drying system in relation to direct electrification of heating processes or other processes that utilize biomass.

Role of the funding source

The funders had no role in the design of the study; in the collection, analysis, and interpretation of data; in the writing of the report; and in the decision to submit the article for publication.

Funding

This work was funded through European Regional Development Fund (ERDF) by the Council of Tampere Region in the project Hiilimetsätalous (Carbon forestry).

CRediT authorship contribution statement

Tomi Thomasson: Conceptualization, Methodology, Software, Formal analysis, Visualization, Writing – Original Draft. **Jyrki Raitila:** Conceptualization, Investigation, Data curation, Writing – Review & Editing, Project administration. **Eemeli Tsupari:** Conceptualization, Validation, Writing – Review & Editing.

Declaration of Competing Interest

The authors declare that they have no known competing financial interests or personal relationships that could have appeared to influence the work reported in this paper.

Data Availability

Data will be made available on request.

References

AFRY. Selvitys turpeen energiankäytön kehityksestä Suomessa. 2020.
Agostini, A., Giuntoli, J., Boulamanti, A., Marelli, L., 2013. Carbon accounting of forest bioenergy. Conclus. Recomm. a Crit. Lit. Rev. https://doi.org/10.2788/29442.
Centre for Economic Development, Transport and the Environment, Yrityksen kehittämisavustus 2023. https://www.ely-keskus.fi/yrityksen-kehittamisavustus.
Colak, N., Hepbasli, A., 2009. A review of heat pump drying: part 1 - systems, models and studies. Energy Convers. Manag 50, 2180–2186. https://doi.org/10.1016/j.enconman.2009.04.031.
Demirbas, A., 2002. Relationships between heating value and lignin, moisture, ash and extractive contents of biomass fuels. Energy Explor. Exploit. 20, 105–111. https://doi.org/10.1260/014459802760170420.
ENTSO-E. ENTSO-E Transparency Platform 2023. https://transparency.entsoe.eu/.
European Investment Bank Group. Coal Regions in Transition 2020:1–4. https://energy.ec.europa.eu/topics/oil-gas-and-coal/eu-coal-regions/coal-regions-transition_en.
Fastmarkets FOEX. PIX Forest Biomass Finland Index History 2020. https://www.fastmarkets.com/commodity-prices/pix-forest-biomass-finland-fp-wb-0003.
Finnish Government. The act banning the use of coal for energy generation in 2029 to enter into force in early April 2019:3–4. https://valtioneuvosto.fi/en/-/1410

877/kivihiilen-energiakayton-vuonna-2029-kieltava-laki-voimaan-huhtikuun-alussa.

Finnish Meteorological Institute. Havaintojen lataus 2023. https://www.ilmatieteenlaitos.fi/havaintojen-lataus.

Francik, S., Łapczyńska-Kordon, B., Francik, R., Wójcik, A., 2018. Model. Simul. Biomass-.-. Dry. Using Artif. Neural Netw. 571–581. https://doi.org/10.1007/978-3-319-72371-6_56.

Gebgeegziabher, T., Oyedun, A.O., Zhang, Y., Hui, C.W., 2013. Effective optimization model for biomass drying. Comput. Aided Chem. Eng. 32, 97–102. https://doi.org/10.1016/B978-0-444-63234-0.50017-8.

IEA. Bioenergy 2023. https://www.iea.org/fuels-and-technologies/bioenergy.

International Organization for Standardization, 2014. EN ISO 17225-1:2014 Solid biofuels. Fuel specifications and classes. Gen. Requir.

Ke, G., Meng, Q., Finley, T., Wang, T., Chen, W., Ma, W., et al., 2017. LightGBM: A highly efficient gradient boosting decision tree. vol. 2017- Decem Adv. Neural Inf. Process Syst. 3147–3155.

Khouya, A., 2021. Modelling and analysis of a hybrid solar dryer for woody biomass. Energy 216. https://doi.org/10.1016/j.energy.2020.119287.

Khouya, A., 2022. Energy analysis of a combined solar wood drying system. Sol. Energy 231, 270–282. https://doi.org/10.1016/j.solener.2021.11.068.

Krigstin, S., Wetzel, S., 2016. A review of mechanisms responsible for changes to stored woody biomass fuels. Fuel 175, 75–86. https://doi.org/10.1016/j.fuel.2016.02.014.

Kumar, B., Szepesi, G., Szamosi, Z., Krámer, G., 2023. Analysis of a combined solar drying system for wood-chips, sawdust, and pellets. Sustain. (Switz.) 15. https://doi.org/10.3390/su15031791.

Li, J., Zhang, Y., Li, M., Wang, Y., Shi, M., Gao, M., et al., 2021. Study on heating performance of solar-assisted heat pump drying system under large temperature difference. Sol. Energy 229, 148–161. https://doi.org/10.1016/j.solener.2021.08.038.

Lund, H., Skov, I.R., Thellufsen, J.Z., Sorknæs, P., Korberg, A.D., Chang, M., et al., 2022. The role of sustainable bioenergy in a fully decarbonised society. Renew. Energy 196, 195–203. https://doi.org/10.1016/j.renene.2022.06.026.

Mandley, S.J., Daioglou, V., Junginger, H.M., van Vuuren, D.P., Wicke, B., 2020. EU bioenergy development to 2050. Renew. Sustain. Energy Rev. 127 https://doi.org/10.1016/j.rser.2020.109858.

Moheno-Barrueta, M., Tzuc, O.M., Martínez-Pereyra, G., Cardoso-Fernández, V., Rojas-Blanco, L., Ramírez-Morales, E., et al., 2021. Experimental evaluation and theoretical optimization of an indirect solar dryer with forced ventilation under tropical climate by an inverse artificial neural network. Appl. Sci. (Switz.) 11. https://doi.org/10.3390/app11167616.

Pang, S., Mujumdar, A.S., 2010. Drying of woody biomass for bioenergy: drying technologies and optimization for an integrated bioenergy plant. Dry. Technol. 28, 690–701. https://doi.org/10.1080/07373931003799236.

Raitila, J., Tsupari, E., 2020. Feasibility of solar-enhanced drying of woody biomass. Bioenergy Res 13, 210–221. https://doi.org/10.1007/s12155-019-10048-z.

Schipfer, F., Mäki, E., Schmieder, U., Lange, N., Schildhauer, T., Hennig, C., et al., 2022. Status of and expectations for flexible bioenergy to support resource efficiency and to accelerate the energy transition. Renew. Sustain. Energy Rev. 158 https://doi.org/10.1016/j.rser.2022.112094.

Sharma, A., Chen, C.R., Vu Lan, N., 2009. Solar-energy drying systems: a review. Renew. Sustain. Energy Rev. 13, 1185–1210. https://doi.org/10.1016/j.rser.2008.08.015.

Statista. European Union Emission Trading System (EU-ETS) carbon pricing 2023. https://www.statista.com/statistics/1322214/carbon-prices-european-union-emission-trading-scheme/.

Statistics Finland. Energy prices n.d. https://stat.fi/en/statistics/ehi.

Svoboda, K., Martinec, J., Pohořelý, M., Baxter, D., 2009. Integration of biomass drying with combustion/gasification technologies and minimization of emissions of organic compounds. Chem. Pap. 63, 15–25. https://doi.org/10.2478/s11696-008-0080-5.

Xie, Z., Gong, Y., Ye, C., Yao, Y., Liu, Y., 2021. Numerical analysis and optimization of solar-assited heat pump drying system with waste heat recovery based on TRNSYS. Processes 9. https://doi.org/10.3390/pr9071118.

Xing, X., Wang, R., Bauer, N., Ciais, P., Cao, J., Chen, J., et al., 2021. Spatially explicit analysis identifies significant potential for bioenergy with carbon capture and storage in China. Nat. Commun. 12 https://doi.org/10.1038/s41467-021-23282-x.

Yang, C., Kwon, H., Bang, B., Jeong, S., Lee, U., 2022. Role of biomass as low-carbon energy source in the era of net zero emissions. Fuel 328. https://doi.org/10.1016/j.fuel.2022.125206.

Yao, M., Li, M., Wang, Y., Li, G., Zhang, Y., Gao, M., et al., 2023. Analysis on characteristics and operation mode of direct solar collector coupled heat pump drying system. Renew. Energy 206, 223–238. https://doi.org/10.1016/j.renene.2023.02.016.

Zou, L., Liu, Y., Yu, M., Yu, J., 2023. A review of solar assisted heat pump technology for drying applications. Energy 283. https://doi.org/10.1016/j.energy.2023.129215.